Evidence of dmisteinbergite (hexagonal form of CaAl$_2$Si$_2$O$_8$) in pseudotachylyte: A tool to constrain the thermal history of a seismic event

Fabrizio Nestola,[1,2,*] **Silvia Mittempergher,**[1] **Giulio Di Toro,**[1,3] **Federico Zorzi,**[1] **and Danilo Pedron**[4]

[1]Dipartimento di Geoscienze, Università di Padova, Via Giotto 1, I-35137 Padova, Italy
[2]CNR-IGG, Sezione di Padova, Via Giotto 1, I-35137 Padova, Italy
[3]Istituto Nazionale di Geofisica e Vulcanologia, Via di Vigna Murata 605, 00143 Roma, Italy
[4]Dipartimento di Scienze Chimiche, Università di Padova, Via Marzolo 1, I-35137 Padova, Italy

Abstract

The determination of the maximum temperature achieved by friction melt (T_{melt}) in pseudotachylyte-bearing faults is crucial to estimate earthquake source parameters (e.g., earthquake energy budgets, co-seismic fault strength) on a geological basis. Here we investigated the mineralogy of a pseudotachylyte from the Gole Larghe Fault (Italian Alps) by using X-ray powder diffraction, micro-Raman spectroscopy, and EDS-equipped field emission scanning electron microscopy. In particular, we report the presence of the hexagonal polymorph of CaAl$_2$Si$_2$O$_8$ (dmisteinbergite) in a pseudotachylyte. Published experimental work shows dmisteinbergite can crystallize at 1200–1400 °C by rapid quenching. Therefore, the presence of dmisteinbergite in pseudotachylyte could be a reliable geothermometer for friction melts for which T_{melt} has only as yet been estimated.

Keywords: Pseudotachylyte, earthquake, dmisteinbergite, geothermometer

Introduction

Tectonic pseudotachylyte (solidified friction melt produced during seismic slip) is the only fault rock that records unambiguously the occurrence of seismic ruptures in exhumed faults (Sibson 1975; Cowan 1999). Therefore, pseudotachylytes may potentially be used to constrain fault processes and seismic source parameters during an earthquake (Sibson 1975; Wenk et al. 2000; Hirose and Shimamoto 2005; Di Toro et al. 2005). For example, pseudotachylyte-bearing faults retain information on the earthquake energy budget (Pittarello et al. 2008) or on fault strength during seismic slip (Sibson 1975; Di Toro et al. 2005; Andersen et al. 2008) that is out of the range of seismological investigations (Kanamori and Heaton 2000). However, to determine, for instance, the amount of heat produced during seismic slip, one poorly constrained unknown parameter is the maximum temperature achieved by the friction melt (T_{melt}). The difficulty in estimating T_{melt} arises from the fact that frictional melting is a non-equilibrium process (Bowden and Tabor 1950). Based on the melting temperatures of the single mineral phases of the host rock, it is only possible to estimate the minimum temperature of the melt (Spray 1992). Because melts may undergo further viscous shear heating during seismic slip (melt superheating, Di Toro and Pennacchioni 2005; Nielsen et al. 2008), it follows that T_{melt} could be higher than temperature estimated from melting of single minerals. Pseudotachylytes consist of lithic clasts (i.e., grains that survive melting) suspended in glass-like (glass or cryptocrystalline to microcrystalline) matrix, which includes microlites nucleated during cooling of the melt (Shand 1916; see also Magloughlin and Spray 1992, Snoke et al. 1998, Lin 2008, and Di Toro et al. 2009 for reviews). Given the difficulties highlighted

above, several methods have been used to estimate T_{melt}. These include the composition of the glass (Lin 1994a), the mineralogy of the newly grown microlites [two pyroxene geothermometer, Toyoshima (1990); omphacite-garnet geothermometer, Austrheim and Boundy (1994); plagioclase crystallization, Lin (1994b); olivine crystallization, Obata and Karato (1995); pigeonite crystallization, Camacho et al. (1995); mullite crystallization, Moecher and Brearley (2004); olivine, clino-, and ortho-pyroxene crystallization, Andersen and Austrheim (2006); the volume ratio between lithic clasts and matrix in pseudotachylytes, O'Hara (2001), the distribution of microstructures in pseudotachylyte veins, Di Toro and Pennacchioni (2004); or commonly, the mineralogy of the lithic clasts, Maddock (1983), Boullier et al. (2001)]. Using these methods, estimates of T_{melt} in natural pseudotachylytes range between 750–1750 °C.

Here we have investigated pseudotachylytes from the Gole Larghe Fault (Italian Alps, Di Toro and Pennacchioni 2004) using X-ray powder diffraction (XRPD), micro-Raman spectroscopy (MRS), and EDS-equipped field emission scanning electron microscope (FESEM). Using this multidisciplinary approach, we have identified unambiguously in a pseudotachylyte the presence of the hexagonal polymorph of CaAl$_2$Si$_2$O$_8$ called dmisteinbergite (Chesnokov et al. 1990). Dmisteinbergite, although included in the feldspar group, is quite different in that it has a phyllosilicate crystal structure. Microlites of plagioclase are well known to be one of the most common constituents of the pseudotachylytes (Shand 1916; Philpotts 1964; Sibson 1975; Passchier 1982; Maddock 1983; Macaudière et al. 1985; Magloughlin 1992; Lin 1994b, 2008; Snoke et al. 1998 for several examples; Shimada et al. 2001; Plattner et al. 2003; Caggianelli et al. 2005), but until now, no dmisteinbergite has been identified, probably due to the analytical techniques applied. Dmisteinbergite was originally

* E-mail: fabrizio.nestola@unipd.it

described in pyrometamorphic rocks from naturally burned coal-bearing spoil-heaps (Chelyabinsk coal basin, Russia) (Chesnokov et al. 1990; Sokol et al. 1998 and references therein). However, unpublished data also describe large crystals of dmisteinbergite in association with a zeolite (wairakite, $CaAl_2Si_4O_{12} \cdot 2H_2O$) in a gabbro (Kurumazawa, Japan). Thus, dmisteinbergite apparently can form both from high temperature combined with rapid cooling (Sokol et al. 1998) or hydrothermally (wairakite occurs widely in low-grade metamorphic rocks, sedimentary environments, and hydrothermal areas; Ori et al. 2008 and references therein). Prior to these reports, dmisteinbergite was obtained only in the laboratory under specific conditions. For instance, Abe et al. (1991) demonstrated that dmisteinbergite crystallizes from a supercooled anorthitic melt and at temperatures between 1200–1400 °C. However, Borghum et al. (1993) showed that dmisteinbergite can also grow in hydrothermal conditions, confirming the above finding of such a phase in association with zeolites.

In this work, we report dmisteinbergite from a pseudotachylyte vein. As such a phase can crystallize only under specific conditions of temperature and cooling rate, its occurrence could be a useful temperature marker (possibly approaching T_{melt}) for extrapolating earthquake source parameters from exhumed faults.

GEOLOGICAL SETTING

The pseudotachylyte was collected from the Gole Larghe Fault Zone, which cuts the tonalites of the Adamello batholith (Italian Southern Alps, for details about the fault zone, see Di Toro and Pennacchioni 2005). The fault zone consists of more than 200 sub-parallel cataclasite-pseudotachylyte-bearing faults and was active 30 Ma ago, at 9–11 km depth, 250–300 °C ambient temperature, and under low pore fluid conditions (Di Toro et al. 2005). The pseudotachylytes are associated with cataclasites (cohesive fault rocks formed by fragmented tonalite cemented by epidote, K-feldspar, and minor chlorite) within the host tonalites (plagioclase 48%, quartz 29%, biotite 17%, and K-feldspar 6%) (Di Toro and Pennacchioni 2004; the whole-rock chemical composition of the initial tonalite and of the pseudotachylyte matrix are reported in the same work). The studied sample is a 5–8 mm thick pseudotachylyte fault vein hosted in tonalite (no evidence of cataclasite precursor) and described in detail by Pittarello et al. (2008).

EXPERIMENTAL METHODS

Microstructural investigations were performed on carbon-coated, polished thin sections with a field emission scanning electron microscope (FE-SEM) JSM6500F upgraded to version 7000 and equipped with an energy dispersive X-ray spectroscopy (EDS) analyzer with internal standards for quantitative chemical composition (Istituto Nazionale di Geofisica e Vulcanologia, Rome, INGV, Italy). Backscattered electron (BSE) images were collected at working distance of 10 mm and accelerating voltage of 10 kV; the BSE resolution in these conditions is 4 nm. The EDS electron beam spot size for analysis was 400 nm as estimated by means of Monte Carlo Method simulations.

Powder X-ray diffraction (XRPD) data were obtained by step scanning using an automated diffractometer system (Philips X'Change) with incident- and diffracted-beam soller slit (0.04 rad.). The instrument was equipped with a curved graphite diffracted-beam monochromator and a gas proportional detector. Divergence and antiscatter slits of 1/2° were used so that the irradiated area could be confined to the sample at angles >10 °2θ. A receiving slit of 0.2 mm was used. A long fine focus Cu X-ray tube was operated at 40 kV and 30 mA. Diffraction pattern was obtained using a step interval of 0.02 °2θ with a counting time of 15 s. The scan was performed over the range 3–70 °2θ. The program High Score Plus (PANalytical) was used for phase identification and Rietveld refinement (Rietveld 1967).

The starting structural model of dmisteinbergite was from Takeuchi and Donnay (1959) (ICSD code 26486). A pseudo-Voigt function was employed for the profile shapes. Refined parameters were scale factors, zero-shift, background (Chebyshev function with 6 coefficients), lattice constants, and profile parameters (Gaussian and Lorentzian coefficients). The agreement indices were $R_p = 7.3\%$ and $R_{wp} = 9.9\%$. For dmisteinbergite, $R_{Bragg} = 6.3\%$.

Raman spectra were collected from the same powdered material studied by XRPD with a home-built micro-Raman system, based on a single 320 mm focal length imaging spectrograph, a Triax-320 ISA instrument, equipped with a holographic 1800 g/mm grating and a liquid-nitrogen-cooled CCD detector (Spectrum One ISA Instruments). The excitation source was a Spectra Physics Ar+ laser (Stabilite 2017-06S) operating at 514.5 nm. A Kaiser Optical System holographic notch filter (514.5 nm) was used to reduce the stray-light level. An Olympus BX 40 optical microscope equipped with three objectives, 20×/0.35, 50×/0.75, and 100×/0.90, was optically coupled to the spectrograph. This made it possible to observe the sample with the microscope and then to select particular micrometric regions for Raman analysis. With the 100× objective, the lateral resolution is estimated to be 0.5 μm and the depth of focus between 1–2 μm. To avoid optical damage to the sample, the power of the exciting radiation was maintained between 10 and 50 mW. The Raman spectra were recorded between 147 and 1200 cm⁻¹ with an instrumental resolution of about 2 cm⁻¹.

RESULTS

Under the FE-SEM, the pseudotachylyte vein comprises clasts of quartz and plagioclase, immersed in a cryptocrystalline rock matrix composed of nanometer-sized biotite and plagioclase (as demonstrated by XRPD, see below) and micrometer-scale titanite-rich clusters (Fig. 1). The quartz clasts are rimmed by 500 nm thick, medium-gray Ca-rich layers and by micrometer-thick, dendritic, silica-rich layers (Fig. 1). EDS analysis of the medium-gray layer indicates the presence of a mineral phase with $CaAl_2Si_2O_8$ composition. Due to its identical composition to anorthite, we combined the experimental techniques of X-ray diffraction and Raman spectroscopy to determine that the $CaAl_2Si_2O_8$ phase was dmisteinbergite. Dmisteinbergite is likely also present in the cryptocrystalline pseudotachylyte. In fact, based on the quantitative analysis by the Rietveld method, the volume proportion of dmisteinbergite is too high to be accounted for solely by the thin rims surrounding the quartz grains. However, we could not identify dmisteinbergite in the matrix by Raman spectroscopy due to its small grain size, probably much smaller than the Raman probe size.

The XRPD diffractogram presented in Figure 2 unambiguously indicates the presence of dmisteinbergite with a volume proportion refined by Rietveld analysis (Rietveld 1967) of 18.2 wt%. The match between the XRPD profile of the Gole Larghe Fault dmisteinbergite and that reported in the literature (PDF2 ICDD 74-0814) is excellent (Fig. 2). The unit-cell parameters for dmisteinbergite obtained by indexing the reflections in Figure 2 are $a = 5.1100(2)$ Å, $c = 14.738(1)$ Å, and $V = 333.278$ Å³. The calculated V reported here is 0.7% smaller than that given by Sokol et al. (1998), but this difference can be understood because the latter sample contained a small fraction of Na substituting for Ca. The overall quantitative analysis by the Rietveld method gives (in wt%): 40.5 quartz, 20.5 plagioclase, 18.2 dmisteinbergite, 17.5 biotite, and 3.3 titanite (Fig. 2).

Micro-Raman spectra collected on several pseudotachylyte grains in every case indicate the presence of dmisteinbergite and quartz. In Figure 3, the published spectrum of dmisteinbergite from the RRUFF Raman database (identification code R061075; Downs 2006) is compared to the spectrum collected in this work. At least five peaks match well those of the reference dmistein-
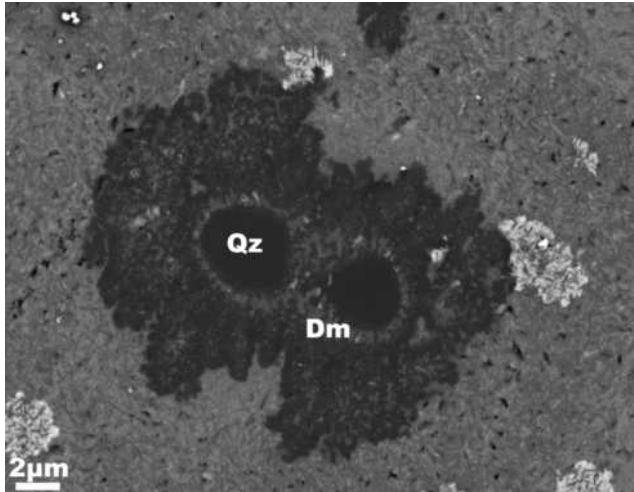
FIGURE 1. Pseudotachylyte from the Gole Larghe Fault. Microstructure of the pseudotachylyte vein: quartz clasts (Qz) are surrounded by a silica-rich, dendritic-like, dark colored halo; the dmisteinbergite (Dm) is the medium gray phase (grains are 200 nm in length) between the quartz clast and the dark halo. The matrix is composed of biotite, plagioclase and aggregates of titanite (bright spots) (BSE, FE-SEM image).

FIGURE 2. X-ray powder diffraction pattern of the Gole Larghe Fault pseudotachylyte. Black line = observed diffraction profile; blue line = calculated diffraction profile by Rietveld refinement; green line = background; red line = difference plot between observed and calculated diffraction profile.

bergite; the observed peaks 329.8, 441.8, 800.6, 895.5, and 913.6 cm^{-1} exactly match the reference peaks 327.9, 439.8, 800.4, 894.4, and 912.3 cm^{-1}, within the 2 cm^{-1} instrument resolution. The remaining peaks of our spectrum clearly belong to quartz (see reference quartz in the same Raman database, code R040031). For purpose of comparison and to show how dissimilar are the Raman spectra of the main phases found in our vein, we also give the main Raman peaks for anorthite (Raman database, code R040059, Downs 2006): 147, 196, 488, 505 (these two are the more intense for anorthite) and 559 cm^{-1}; and for biotite (Wang et al. 1994): 178, 549, 679, 717, 767 (these last three peaks are the more intense for biotite), and 3650 (OH group) cm^{-1}.

DISCUSSION

Before it was identified in nature, dmisteinbergite was studied by several authors as a synthetic phase, and it was demonstrated that it could be obtained under high-temperature conditions and in a supercooled melt (e.g., Abe et al. 1991). Its rarity in nature is likely due to its metastability (Abe and Sunagawa 1995). Nucleation of metastable phases is known for several silicates and they are observed, for example, when a melt is cooled instantaneously or a glass is heated rapidly (Putnis and Bish 1983). Hexagonal form of CaAl$_2$Si$_2$O$_8$ was also synthesized by hydrothermal processing of monocalcium aluminate (CaAl$_2$O$_4$) and quartz at temperatures as low as 200 °C (Borghum et al. 1993), but such ambient conditions are ruled out for a pseudotachylyte produced by frictional melting of tonalite where the temperatures achieved are markedly higher and no monocalcium aluminate is available. Moreover, hydrothermal processing and alteration of the pseudotachylyte should have caused the breakdown of microlites of biotite into chlorite, a breakdown reaction that is not observed in the rocks studied. We consider dmisteinbergite found in this work of high-temperature origin for the following reasons: (1) presence of nano-crystals of dmisteinbergite, which is inconsistent with the hypothesis of a low-temperature and
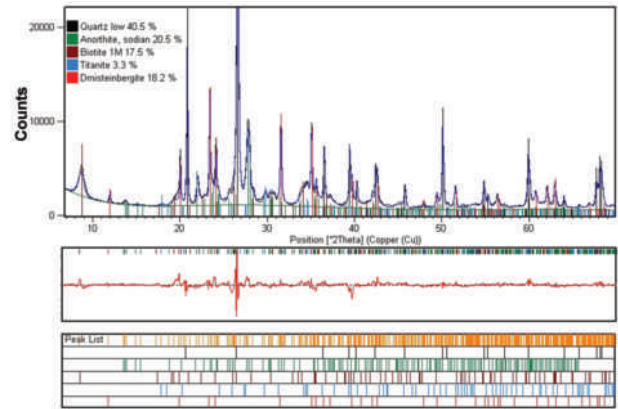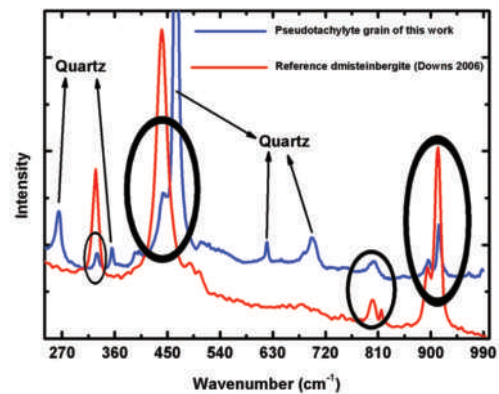

FIGURE 3. Raman spectrum of one grain from the same sample of pseudotachylyte studied by X-ray powder diffraction. Black line = measured spectrum; red line = Raman spectrum of dmisteinbergite (sample R040031, http://rruff.info/, Downs 2006). The ellipses highlight the match between the dmisteinbergite studied in this work and that reported in the RRUFF database.

hydrothermal environment of crystallization (the only reported dmisteinbergite of low temperature in nature is present in crystals of centimeter size), and (2) absence of wairakite or other zeolite-type minerals that are found in association with dmisteinbergite in a hydrothermal environment.

Recent works focused on the high-temperature modifications of CaAl$_2$Si$_2$O$_8$ polymorphs reported by Abe et al. (1991) and Abe and Sunagawa (1995). In those works, the authors investigated a melt of pure anorthitic composition (plus a melt with composition anorthite:wollastonite = 80:20) and a melt with composition anorthite:forsterite:silica = 70:10:20, respectively. Abe et al. (1991) found that the hexagonal form of CaAl$_2$Si$_2$O$_8$ nucleates and grows prior to the appearance of stable anorthite when the melt is supercooled below 1200 °C, has a melting point of 1400 ± 15 °C, and rapidly disappears in the presence of anorthite. Abe and Sunagawa (1995), studying an impure anorthitic composition, found that by supercooling the melt (with a ΔT = 350–400 °C) down to 1100–1000 °C, dmisteinbergite nucleates dominantly instead of anorthite (similar to the An$_{100}$ and An$_{80}$Wo$_{20}$ melts see Abe et al. 1991). In conclusion, they found that the hexagonal form of

$CaAl_2Si_2O_8$ cannot coexist in nature with anorthite. In early work on anorthitic melt compositions (Davis and Tuttle 1951), it was found that rapid quenching of the melt to 1200 °C yields only the hexagonal polymorph. Bruno et al. (1976) also observed that for an anorthitic melt quenched from 1530 °C to room temperature in a few seconds, only anorthite is produced. Based on these experimental results, it appears that the presence of dmisteinbergite in natural pseudotachylytes could be a reliable indicator of high-temperature conditions and extremely rapid quenching.

The direct extrapolation of experimental results to natural conditions is not straightforward. First, the bulk composition of the pseudotachylyte precursor (i.e., tonalite or cataclasite in the case of the Gole Larghe Fault zone) is not pure anorthite. However, the high-temperature experiments on the hexagonal form of $CaAl_2Si_2O_8$ were also performed on impure anorthitic composition, yielding similar results (Abe and Sunagawa 1995). Therefore, the temperature of the polymorphic transformation of $CaAl_2Si_2O_8$ does not depend upon the initial bulk composition of the melt but only on the temperature and on the rate of supercooling. Second, the pseudotachylyte from the Gole Larghe Fault Zone was produced at 10 km depth (which corresponds to a confining pressure of 0.25 GPa) and probably under low pore pressures (Di Toro and Pennacchioni 2004; Di Toro et al. 2005). However, Morse (1980) showed that the confining pressure (at least up to 1 GPa) does not have any effect on the melting point for a pure anorthite and it increases the melting point by only 10–15 °C for $An_{80}Ab_{20}$ compositions. Third, dmisteinbergite has a crystal structure (i.e., sheet silicate) totally distinct from that of anorthite (Ito 1976). This implies that the transformation from dmisteinbergite to anorthite must be reconstructive (i.e., breaking and formation of new chemical bonds), a type of lattice rearrangement that requires high activation energies and transition times on the order of minutes.

The sample studied was extracted from a pseudotachylyte-bearing fault vein that was 8 mm thick. In the case of an 8 mm thick melt layer with an initial temperature of 1450 °C and hosted in a rock at 250 °C, thermal modeling suggests that cooling rates can be as large as 100–200 °C/s approaching the center of the vein (at the vein margins cooling to about half of the initial temperature of the melt is almost instantaneous: see Di Toro and Pennacchioni 2004 for thermal modeling details). It follows that the dmisteinbergite was preserved in the pseudotachylyte because the lattice rearrangement to anorthite would have required longer times to transform (Abe and Sunagawa 1995). The finding of dmisteinbergite suggests T_{melt} close to 1400 °C, consistent with the previous estimate of 1450 °C based on the distribution of the microstructures in the pseudotachylyte (Di Toro and Pennacchioni 2004). However, the previous T_{melt} estimate was based on many assumptions and time consuming microstructural work.

This is only the third reported occurrence of dmisteinbergite in nature; therefore, it would appear that dmisteinbergite cannot be a useful thermal marker because of its rarity. In addition, to identify this mineral several analytical techniques in combination are required. However, given the small grain size, we suggest that dmisteinbergite may not be so rare, but rather that its abundance is simply underestimated. We expect dmisteinbergite is probably more common than reported in rocks produced during large thermal pulses (e.g., seismic faulting, but also meteorite impacts).

REFERENCES CITED

Abe, T. and Sunagawa, I. (1995) Hexagonal $CaAl_2Si_2O_8$ in a high-temperature solution; metastable crystallization and transformation to anorthite. Mineralogical Journal, 17, 257–281.

Abe, T., Tsukamoto, K., and Sunagawa, I. (1991) Nucleation, growth and stability of $CaAl_2Si_2O_8$ polymorphs. Physics and Chemistry of Minerals, 17, 473–484.

Andersen, T.B. and Austrheim, H. (2006) Fossil earthquakes recorded by pseudotachylytes in mantle peridotite from the Alpine subduction complex of Corsica. Earth and Planetary Science Letters, 242, 58–72.

Andersen, T.B., Mair, K., Austrheim, H., Podladchikov, Y.Y., and Vrijmoed, J.C. (2008) Stress release in exhumed intermediate and deep earthquakes determined from ultramafic pseudotachylyte. Geology, 36, 995–998.

Austrheim, H. and Boundy, T.M. (1994) Pseudotachylytes generated during seismic faulting and eclogitization of the deep crust. Science, 265, 82–83.

Borghum, B.P., Bukowski, J.M., and Young, J.F. (1993) Low-temperature synthesis of hexagonal anorthite via hydrothermal processing. Journal of the American Ceramic Society, 76, 1354–1356.

Boullier, A.M., Ohtani, T., Fujimoto, K., Ito, H., and Dubois, M. (2001) Fluid inclusions in pseudotachylytes from the Nojima fault, Japan. Journal of Geophysical Research, 106, 21965–21977.

Bowden, F.P. and Tabor, D. (1950) The Friction and Lubrication of Solids, 374 p. Clarendon Press, Oxford.

Bruno, E., Chiari, G., and Facchinelli, A. (1976) Anorthite quenched from 1530 °C. Structure refinement. Acta Crystallographica, B32, 3270–3280.

Caggianelli, A., De Lorenzo, S., and Prosser, G. (2005) Modeling the heat pulses generated on a fault plane during coseismic slip: Inferences from the pseudotachylytes of the Copanello cliffs (Calabria, Italy). Tectonophysics, 405, 99–119.

Camacho, A., Vernon, R.H., and Fitz Gerald, J.D. (1995) Large volumes of anhydrous pseudotachylyte in the Woodroffe Thrust, eastern Musgrave Ranges, Australia. Journal of Structural Geology, 17, 371–383.

Chesnokov, B.V., Lotova, E.V., Nigmatulina, E.N., Pavlyuchenko, V.S., and Bushmakin, A.F. (1990) Dmisteinbergite $CaAl_2Si_2O_8$ (hexagonal)—A new mineral. Zapiski Vsesoyuz Mineralogicheskogo Obshchestva, 119, 43–45.

Cowan, D.S. (1999) Do faults preserve a record of seismic faulting? A field geologist's opinion. Journal of Structural Geology, 21, 995–1001.

Davis, G.L. and Tuttle, O.F. (1951) Two new crystalline phases of the anorthite composition, $CaO·Al_2O_3·SiO_2$. American Journal of Sciences, Bowen Volume, 107–114.

Di Toro, G. and Pennacchioni, G. (2004) Superheated friction-induced melts in zoned pseudotachylytes within the Adamello tonalites (Italian Southern Alps). Journal of Structural Geology, 26, 1783–1801.

——— (2005) Fault plane processes and mesoscopic structure of a strong-type seismogenic fault in tonalites (Adamello batholith, Southern Alps). Tectonophysics, 402, 54–79.

Di Toro, G., Pennacchioni, G., and Teza, G. (2005) Can pseudotachylytes be used to infer earthquake source parameters? An example of limitations in the study of exhumed faults. Tectonophysics, 402, 3–20.

Di Toro, G., Pennacchioni G., and Nielsen, S. (2009) Pseudotachylytes and earthquake source mechanics. In E. Fukuyama, Ed., Fault-zone Properties and Earthquake Rupture Dynamics, p. 87–133. International Geophysics Series, Elsevier, Amsterdam.

Downs, R.T. (2006) The RRUFF Project: An integrated study of the chemistry, crystallography, Raman and infrared spectroscopy of minerals. Program and Abstracts of the 19th General Meeting of the International Mineralogical Association in Kobe, Japan. O03-13.

Hirose, T. and Shimamoto, T. (2005) Slip-weakening distance of faults during frictional melting as inferred from experimental and natural pseudotachylytes. Bulletin of the Seismological Society of America, 95, 1666–1673.

Ito, J. (1976) High temperature solvent growth of anorthite on the join $CaAlSi_2O_8$-SiO_2. Contributions to Mineralogy and Petrology, 59, 187–194.

Kanamori, H. and Heaton, T.H. (2000) Microscopic and macroscopic physics of earthquakes. In J. Rundle, D.L. Turcotte, and W. Klein, Eds., Geocomplexity and the Physics of Earthquakes, 120, p. 147–163. AGU Monograph Series, Washington, D.C.

Lin, A. (1994a) Glassy pseudotachylytes from the Fuyun Fault Zone, Northwest China. Journal of Structural Geology, 16, 71–83.

——— (1994b) Microlite morphology and chemistry in pseudotachylyte, from the Fuyun Fault Zone, Northwest China. Journal of Geology, 102, 317–329.

——— (2008) Fossil Earthquakes: The Formation and Preservation of Pseudotachylytes, 348 p. Springer, Berlin.

Macaudière, J., Brown, L.W., and Ohnenstetter, D. (1985) Microcrystalline textures resulting from rapid crystallization in a pseudotachylite melt in a meta-anorthosite. Contribution to Mineralogy and Petrology, 89, 39–51.

Maddock, R.H. (1983) Melt origin of fault-generated pseudotachylytes demonstrated by textures. Geology, 11, 105–108.

Magloughlin, J.F. (1992) Microstructural and chemical changes associated with cataclasis and frictional melting at shallow crustal levels: The cataclasite-pseudotachylyte connection. Tectonophysics, 204, 243–260.

Magloughlin, J.F. and Spray, J.G. (1992) Frictional melting processes and products in geological materials: introduction and discussion. Tectonophysics, 204, 197–206.

Moecher, D.P. and Brearley, A.J. (2004) Mineralogy and petrology of a mullite-bearing pseudotachylyte: Constraints on the temperature of coseismic frictional fusion. American Mineralogist, 89, 1486–1495.

Morse, S.A. (1980) Basalts and Phase Diagrams, p. 493. Springer-Verlag, New York.

Nielsen, S., Di Toro, G., Hirose, T., and Shimamoto, T. (2008) Frictional melt and seismic slip. Journal of Geophysical Research, 113, B01308, DOI: 10.1029/2007JB005122.

Passchier, C.W. (1982) Pseudotachylyte and the development of ultramylonite bands in the Saint-Barthelémy Massif, French Pyrenees. Journal of Structural Geology, 4, 69–79.

Philpotts, A.R. (1964) Origin of Pseudotachylites. American Journal of Science, 262, 1008–1035.

Plattner, U., Markl, G., and Sherlock, S. (2003) Chemical heterogeneities of Caledonian (?) pseudotachylites in the Eidsfjord Anorthosite, north Norway. Contributions to Mineralogy and Petrology, 145, 316–338.

Obata, M. and Karato, S. (1995) Ultramafic pseudotachylyte from the Balmuccia peridotite, Ivrea-Verbano zone, Northern Italy. Tectonophysics, 242, 313–328.

O'Hara, K. (2001) A pseudotachylyte geothermometer. Journal of Structural Geology, 23, 1345–1357.

Ori, S., Quartieri, S., Vezzalini, G., and Dmitriev, V. (2008) Pressure-induced structural deformation and elastic behavior of wairakite. American Mineralogist, 93, 53–62.

Pittarello, L., Di Toro, G., Bizzarri, A., Pennacchioni, G., Hadizadeh, J., and Cocco, M. (2008) Energy partitioning during seismic slip in pseudotachylyte-bearing faults (Gole Larghe Fault, Adamello, Italy). Earth and Planetary Science Letters, 269, 131–139.

Putnis, A. and Bish, D.L. (1983) The mechanism and kinetics of Al,Si ordering in Mg-cordierite. American Mineralogist, 68, 60–65.

Rietveld, H.M. (1967) Line profiles of neutron powder-diffraction peaks for structure refinement. Acta Crystallographica, 22, 151–152.

Shand, S.J. (1916) The pseudotachylyte of Parijs (Orange Free State) and its relation to "trap-shotten gneiss" and "flinty crush-rock." Quarterly Journal of the Geological Society of London, 72, 198–221.

Shimada, K., Kobari, Y., Okamoto, T., Takagi, H., and Saka, Y. (2001) Pseudotachylyte veins associated with granitic cataclasite along the Median Tectonic Line, eastern Kii Peninsula, Southwest Japan. The Journal of the Geological Society of Japan, 107, 117–128.

Sibson, R.H. (1975) Generation of pseudotachylyte by ancient seismic faulting. Geophysical Journal of the Royal Astronomical Society, 43, 775–794.

Snoke, A.W., Tullis, J., and Todd, V. (1998) Fault-related Rocks. A Photographic Atlas, p. 617. Princeton University Press, New Jersey.

Sokol, E., Volkova, N., and Lepezin, G. (1998) Mineralogy of pyrometamorphic rocks associated with naturally burned coal-bearing spoil-heaps of the Chelyabinsk coal basin, Russia. European Journal of Mineralogy, 10, 1003–1014.

Spray, J.G. (1992) A physical basis for the frictional melting of some rock-forming minerals. Tectonophysics, 204, 205–221.

Takeuchi, Y. and Donnay, G. (1959) The crystal structure of hexagonal $CaAl_2Si_2O_8$. Acta Crystallographica, 12, 465–470.

Toyoshima, T. (1990) Pseudotachylite from the Main Zone of the Hidaka metamorphic belt, Hokkaido, northern Japan. Journal of Metamorphic Geology, 8, 507–523.

Wang, A., Han, J., Guo, L., Yu, J., and Zeng, P. (1994) Database of standard Raman spectra of minerals and related inorganic crystals. Applied Spectroscopy, 48, 959–968.

Wenk, H.R., Johnson, L.R., and Ratschbacher, L. (2000) Pseudotachylites in the Eastern Peninsular Ranges of California. Tectonophysics, 321, 253–277.